

# Environmental Science

*An Indian Journal*

*Current Research Paper*

ESAIJ, 10(9), 2015 [326-337]

## Porosity analysis using image logs

Mostafa Alizadeh\*, Zohreh Movahed, Radzuan Bin Junin

Faculty of Petroleum and Renewable Energy Engineering Universiti Teknologi Malaysia, 81310 UTM Johor Bahru, Johor, (MALAYSIA)

E-mail: mostafa.alizadeh88@yahoo.com, zmovahed@gmail.com, radzuan@petroleum.utm.my

### ABSTRACT

Porosity analysis is the way to have a better understanding of porosity system in oil and gas fields. By using the image log technology, we can do this analysis very well, but this process is complicated and it is still unknown to many researchers. Therefore, we decided to explain this process by using a unique case study and a number of valuable image log interpretation examples. This job will be done for two wells (GS-A & GS-B) located in Gachsaran field, one of the most important Iranian fields, and the main reservoir that will be studied is Asmari reservoir, one of the most important Iranian oil and gas reservoirs. We aim to offer a unique educational paper that will be very useful for the other researchers who are interested in image log technology. © 2015 Trade Science Inc. - INDIA

### KEYWORDS

Porosity analysis;  
Oil and gas reservoirs;  
Image log technology.

### INTRODUCTION

Gachsaran oil field is in the southwest of Iran Figure 1 with an anticline structure, made of anhydrite/salt, 80 km long, 300m-1500m thickness, 8-18 km wide; it provides an excellent seal for the Asmari reservoir, the Pabdeh reservoir, the Gurpi reservoir and the other reservoirs Figure 2<sup>[1]</sup>.

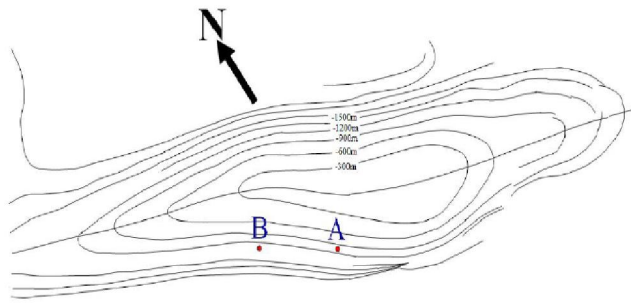
Most carbonate formation evaluation methods rely on traditional resistivity and porosity logs. For many carbonate reservoirs, the correlation between hydrocarbon production and density-neutron logs has been inconsistent. Good production has been obtained from intervals where logs show low porosity whereas zones having higher porosity have not produced. Total production from carbonate reservoirs in mature fields has often been greater than expected from standard porosity logs<sup>[2]</sup>.

Many productive carbonates have complex dual porosity systems with widely varying proportions of primary and secondary porosity. The secondary porosity may contain vugs, moulds (oo moulds or biomoulds), channels, and fractures. Moreover, the originally homogeneous matrix / intergranular primary porosity may become patchy through selective cementation of the matrix. On the conventional porosity logs (density, neutron, and sonic), these porosity types often appear somewhat uniformly distributed. Moreover, due to coarse resolution of the conventional tools, such types of porosity get under-estimated or overlooked<sup>[3]</sup>.

Borehole electrical images, FMI (Formation Micro Imager) in particular, provide both high resolution and azimuthal borehole coverage to resolve quantitatively the heterogeneous nature of porosity



(a)



(b)

**Figure 1 : (a) Location of the Gachsaran field; (b) UGC map of the Gachsaran field and the studied wells (GS-A & GS-B)**

components.

In this work, 2 wells located in Gachsaran oil field will be selected, and the porosity analysis will be done in these wells by using the image logs and the other geological logs interpretation. We will do the porosity analysis in order to both having a better understanding of porosity system in this field and also explaining the methodology by showing the selected log interpretation examples from this field.

## MATERIALS & METHODS

Borehole imaging delivers micro resistivity and acoustic images of the formation in both water-based and nonconductive mud. Borehole imaging is the preferred approach for determining net pay in the laminated sediments of fluvial and turbidite depositional environments<sup>[4]</sup>.

The FMI has a four-arm eight-pad array (i.e., four pads and four flaps as shown in Figure 3 Each pad and flap contains 24 buttons to make 192 buttons total for all four pads and four flaps. The tool includes a general purpose inclinometer cartridge,

which provides accelerometer and magnetometer data. The tri-axial accelerometer gives speed determination and allows re-computation of the exact position of the tool. The magnetometers determine tool orientation. During logging, each microelectrode emits a passive, focused current into the formation Figure. The current intensity measurements, which reflect micro resistivity variations, are converted to variable-intensity gray or color images. The observation and analysis of the images provide information related to changes in rock composition, texture, structure or fluid content Figure 3.

Schlumberger company has introduced a new approach to utilize borehole electrical images in the analysis of carbonate reservoirs' porosity system. Through this technique porosity distribution and quantity of vugs / moulds fraction can be obtained. However, the results of the technique are affected largely by shale and bad hole conditions. In case the quality of one or two images is largely affected due to damaged FMI pad / flap or bad hole, such images can be discarded during the analysis.

The primary assumption for this technique is that the resistivity data from the electrical images is measured in the flushed zone of the borehole. The electrical images are then transformed into a porosity map of the borehole after their calibration with the shallow resistivity and log porosity (preferably effective porosity). Following equation is used to get such transformation; it takes log porosity (effective log porosity being the best option), any shallow resistivity measurement (mostly LLS or SFLU), and conductivity of individual FMI electrodes / buttons ( $C_i$ ) as inputs.

$$(\phi)_{fmi} = (\phi)_{log} * [LLS * C_i]^{1/m}$$

(Where  $C_i$  is conductivity of each FMI electrodes,  $m$  is cementation factor, and  $\phi_{log}$  is log porosity)

For the study well, synthetic average FMI resistivity (SRES) was used as resistivity and PXND (porosity derived from crossplot density-neutron logs) as log porosity to be input into the above equation. Ideally effective log porosity should be used which is derived from the log analysis. Since no log analysis was carried out, therefore simple cross-plot neutron-density porosity was used for the study well. The cementation factor ( $m$ ) was used as 1.9 for the

Current Research Paper

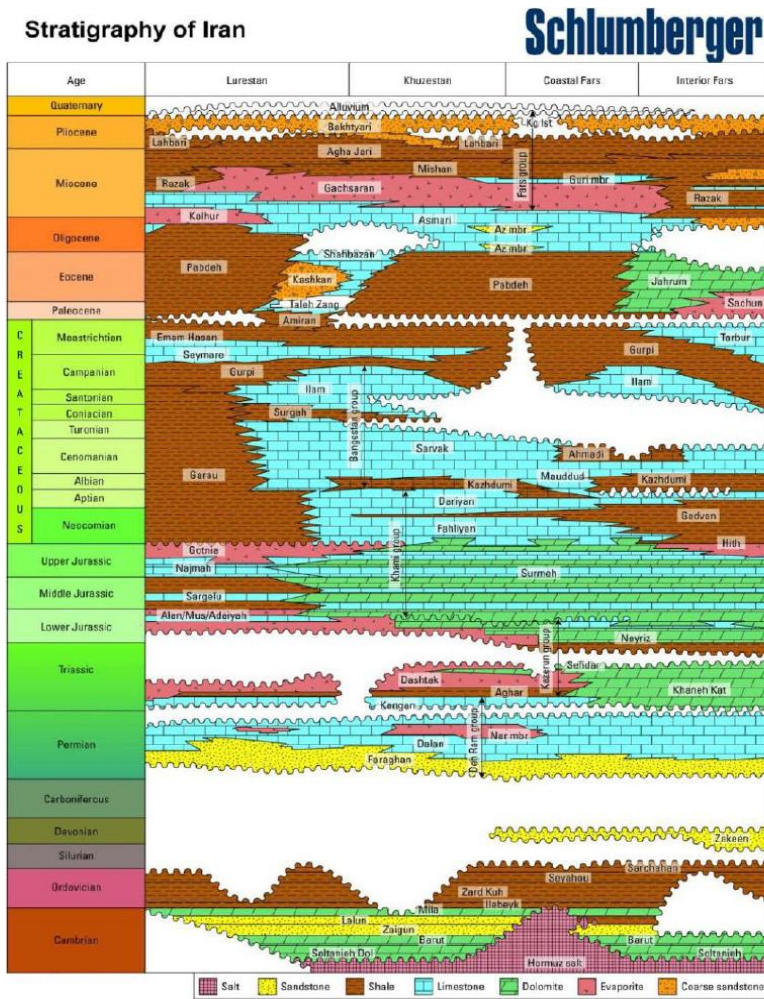


Figure 2 : Picture showing the Gachsaran field overlying the Asmari, Pabdeh, Gurpi and other reservoirs, and stratigraphic nomenclature of rock units and age relationships in the Zagros basin

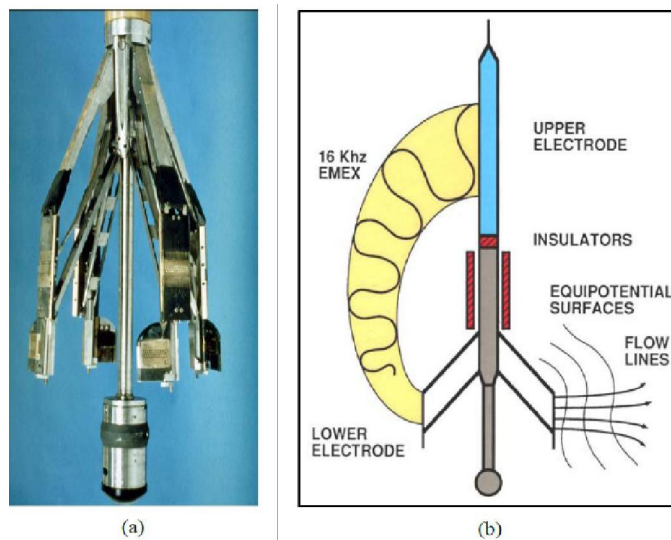


Figure 3 : (a) Picture of FMI tool (b) explanation of the principle of measurement. EMEX current flows into the formation from the FBCC (upper electrodes) housing to pad section (which is the FMI sonde section carrying 192 imaging micro-electrodes), called lower electrode

whole interval of each formation. Automated analysis of this porosity map, windowed over short intervals (generally 1.2 inch), provides a continuous output of primary and macro-secondary porosity components of rocks. At every specified sampling rate (generally 0.1 inch for oomouldic porosity system or 0.3 inch or bigger for formations having large size vugs or moulds), porosity distribution histograms are computed. The homogeneous carbonate intervals give narrow unimodal distribution Figures 4 & 5.

In vuggy carbonates, highly skewed unimodal or bimodal distribution of porosity is observed. While in the most heterogeneous carbonates where cementation, primary porosity and vuggy porosity are present,

highly skewed and broad or bimodal / trimodal porosity distribution may be observed. On such histograms, the points from the high porosity ends represent leached pores (vugs or moulds) and fracture fractions of porosity. Whereas the points from the low porosity end belong to the dense or cemented areas of the host rock (Figure 6).

The area under the high porosity tails of porosity histograms gives quantity of secondary porosity. A continuous / moving threshold or cutoff is applied to the porosity histograms to separate the contribution of secondary pores from the host pore fraction, which may be comprised of primary interparticle / intraparticle pores and secondary micro-pores (that are

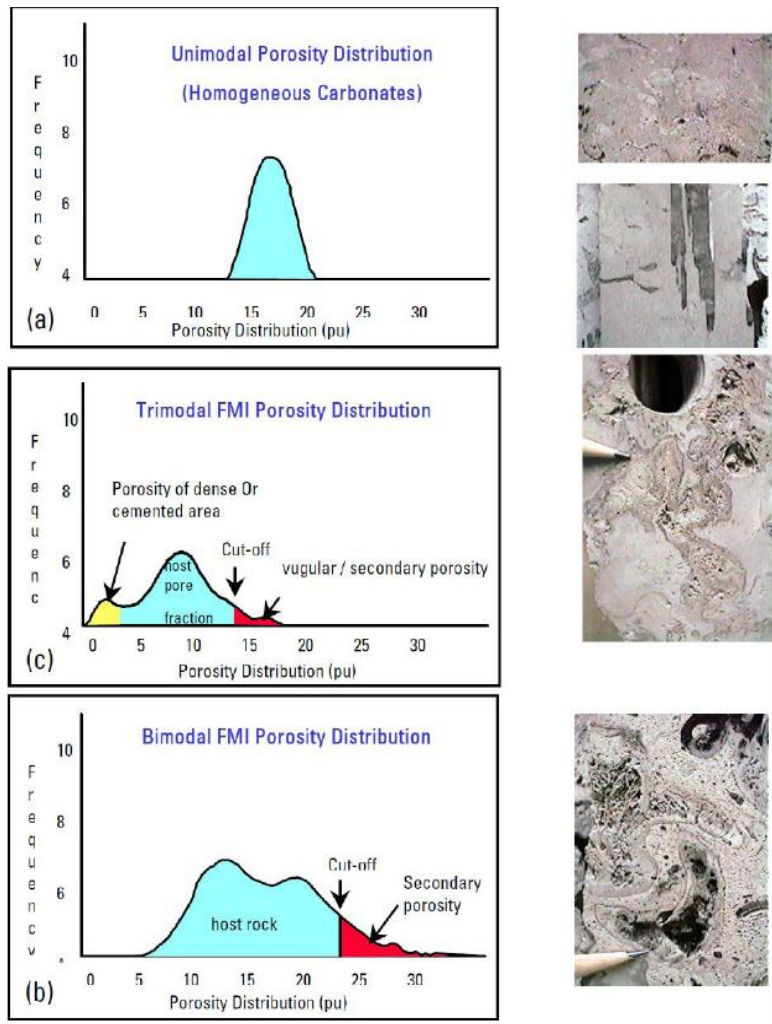


**Figure 4 : Explanation of the method used for porosity analysis from FMI and logs. Typical FMI porosity histograms showing porosity distributions in homogeneous and heterogeneous carbonates. Unimodal distribution is found in homogeneous carbonates (a). While bimodal to trimodal distributions are found in heterogeneous carbonates (b & c). The porosity component due to vugs and fractures is obtained by applying an empirical cut-off to the porosity histograms**

## Current Research Paper

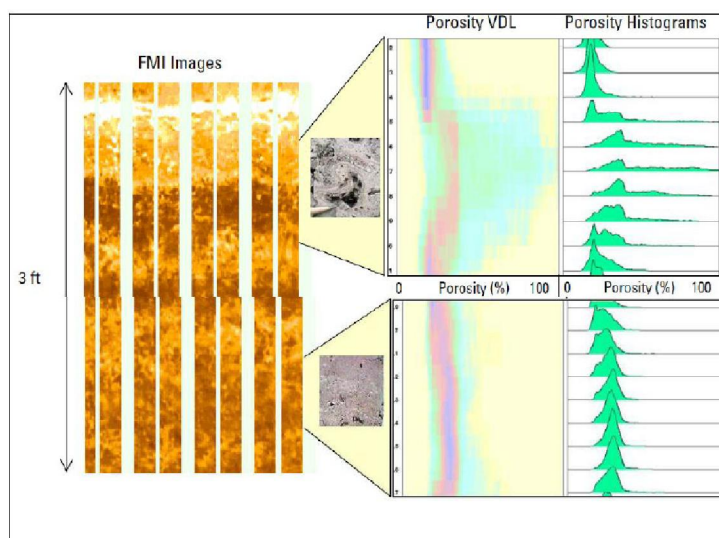


**Figure 5 :** Example of porosity analysis from FMI and Logs showing difference in vuggy and non-vuggy sections of a rock. Two small sections of FMI are transformed into porosity domain, which is shown as porosity histograms and variable density display developed from a series of porosity histograms

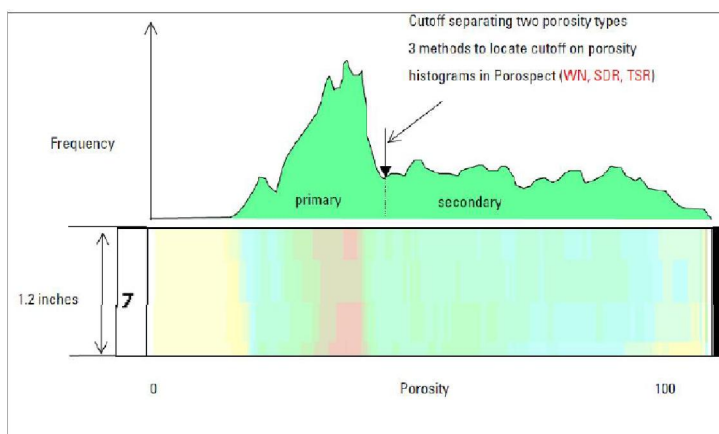


**Figure 6 :** Figure explaining porosity VDL generation from Porosity histograms. Expanded view of a section from Figure 17 (indicated with a black bar) to explain relationship between porosity histograms and variable density display (VDL). The maximum porosity points are shown in magenta, which corresponds to high frequency section of porosity histogram. The cutoff indicates the boundary between matrix (and intergranular and intra-granular porosity) and macro secondary pores (leached pores of different origin in the present study). The area under the high porosity tail beyond the cutoff gives amount of macros secondary pores

not seen by the FMI). So the porosity points above the threshold correspond to the macro-secondary pores and the one below correspond to host pores. There are three different types of thresholds / cutoffs that are applied to the porosity data. The description of each method is given below:

### WN Threshold Method

In this method, first the standard deviation of the histogram below the median porosity is computed. Then the cutoff / threshold is obtained by adding a multiple of this standard deviation to the median poros-

ity. Generally the value of the multiple is taken as 3; however this is not fixed. It can be increased or decreased based on the calibration of the porosity results with cores.

### SDR or Fixed-Percentage Threshold Method

This is a variant of WN method. It locates the threshold at a fixed percentage (typically 15 %) above the mean porosity. The percentage value is not fixed. It may be greater or smaller than 15 %. Core observation / measurement provides a way to fix its value.

### TSR or Discriminant Threshold

This method does not require any user input to define the threshold. It involves the use of Discriminant Threshold Selection Algorithm, which is based on the standard linear discriminant analysis used in the field of pattern recognition and statistics. This method works on the idea that if the porosity data consists of two populations, then the best threshold should maximally separate the two means.

Average of the overall porosity seen collectively by all (192) FMI buttons / electrodes is also computed. Across the homogeneous carbonate intervals, which compute unimodal porosity distribution, the average of the image porosity reads nearly the same as the effective log porosity. The unimodal porosity distribution changes into bimodal or trimodal or broad distribution across the heterogeneous carbonate intervals. The average image porosity across such intervals may be either more or less than the effective log porosity depending upon the type of heterogeneity, i.e., dense areas, vugs, moulds, fractures, matrix patches of very high porosity, dense streaks or high porosity streaks.

**Porosity analysis for the well number GS-A**

**(a) Porosity system**

The accuracy of porosity analysis from the image logs is largely dependent on the selection of right values for the parameters used in the analysis. Therefore some priori knowledge about the type and size of secondary pores is required for the rocks to be evaluated with the imaging tools. Since no core data was available for that purpose in the study well, therefore analysis was carried out in such a way that whole range of macro-secondary pores could be addressed. The porosity analysis was carried out to provide macro-secondary porosity (vugs / moulds) and high-resolution porosity for Asmari formation. The porosity results (secondary porosity and high resolution porosity) are output at 0.1 inch and 1.5 inch. While the porosity histogram / VDL display is output at 1.5 inch. All porosity results (secondary porosity, porosity minimum and maximum limits, and high resolution porosity) from the study well are displayed at 1.5 inch in the (Figures 7 & 8). The results

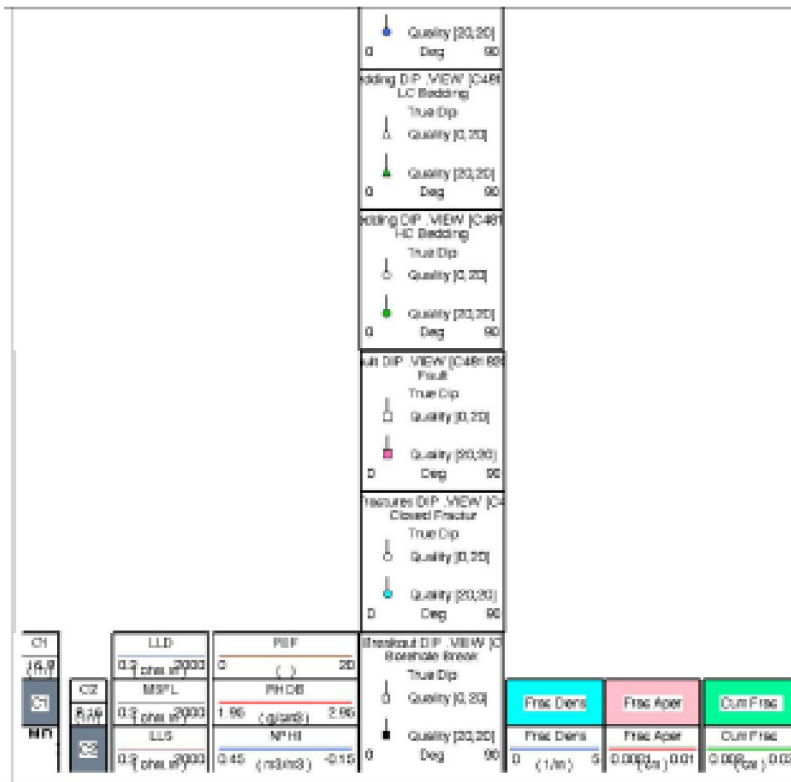


Figure 7 : Header for the summary plot of Figure 8

# Current Research Paper

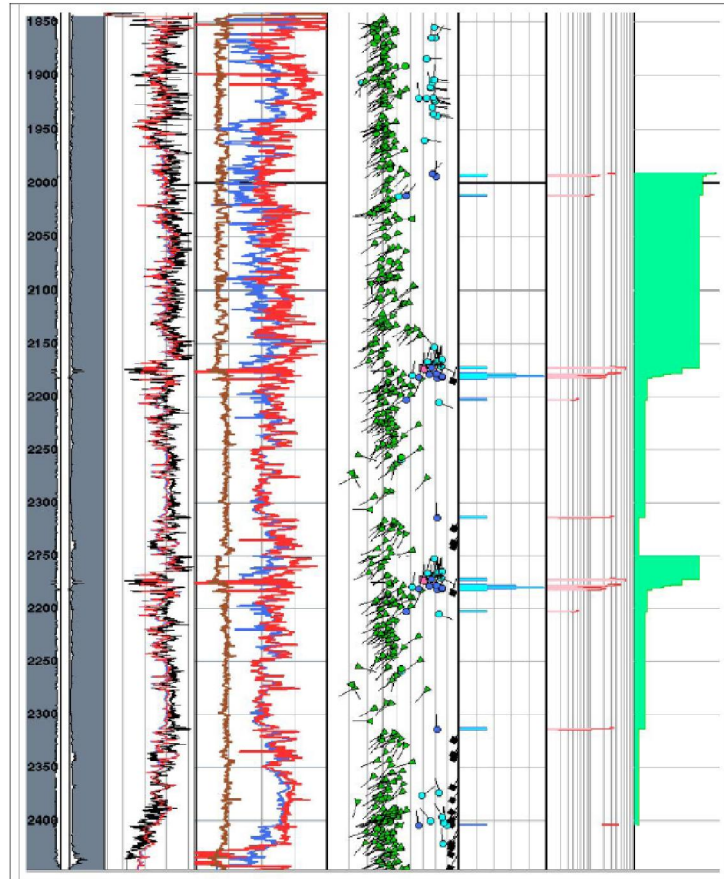


Figure 8 : Summary log of resistivity, density, porosity, dips, open fractures density and apertures in Asmari formation

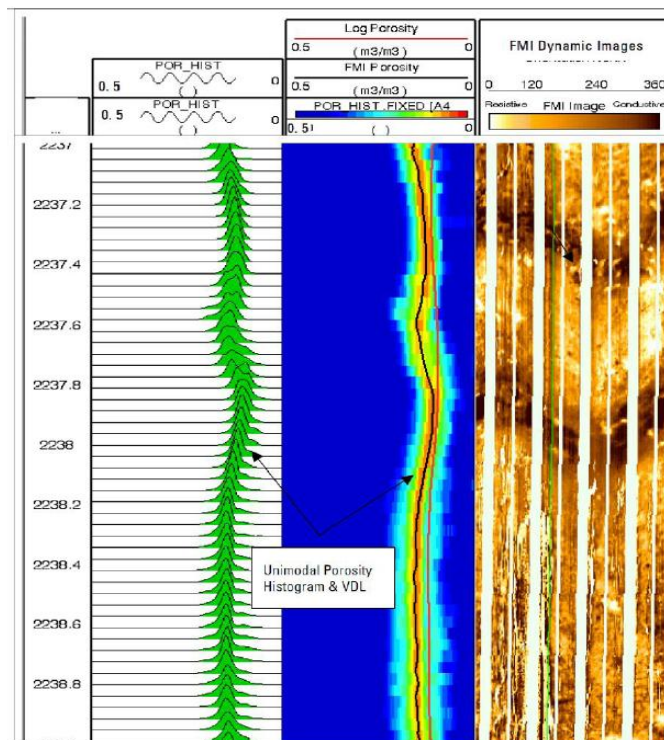
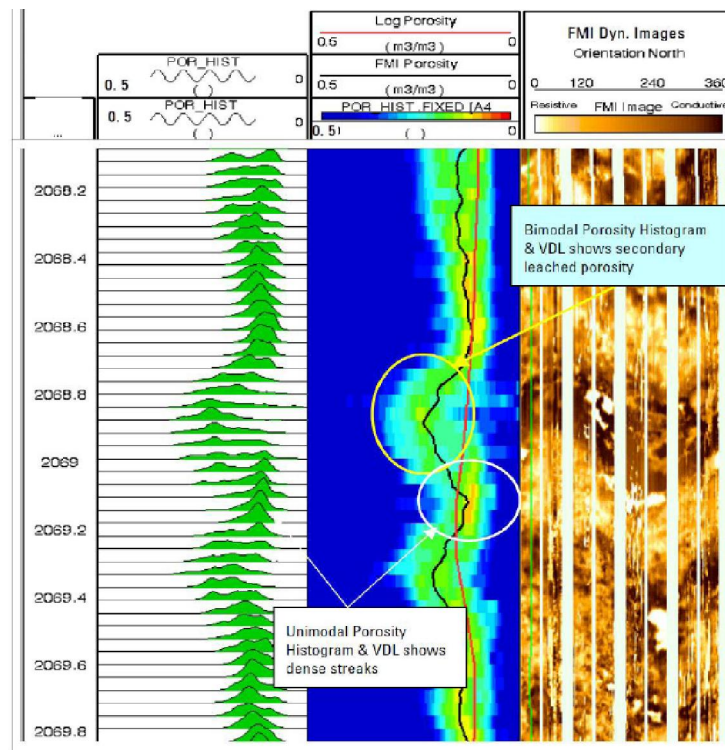


Figure 9 : Narrow range of porosity shown by porosity-VDL (variable-density-log) and porosity-histograms in a section of Asmari indicates its homogeneous nature



**Figure 10 : Porosity VDL (variable-density-log) and histogram display over a section of Asmari Formation showing presence of secondary / leached porosity as indicated by high porosity tails on FMI transformed porosity histograms and VDL displays. FMI images are showing patchy appearance across that section. High and low porosity streaks are also indicated by the high resolution porosity (FMI Porosity) and porosity VDL / histograms**

of porosity analysis are discussed in the following.

### (b) Vuggy / mouldic porosity

As indicated by the higher porosity tails of porosity histograms / VDL, there are some sections in Asmari which appear to be vuggy / mouldic. The vuggy / mouldic porosity (also called secondary porosity in the report to include all components of leached pores) was then computed by applying an optimal dynamic cutoff to the porosity histograms to compute the area under the high porosity tails. A multiplier of 3.0 was used for the WN method and 15% for the SDR method. Previous studies on carbonates, using FMI, logs and cores, indicated that TSR method generally gives better results for secondary porosity computation from porosity VDL / histograms. So it is assumed that secondary porosity estimated by TSR method in the study well is possibly better than the other two threshold methods. However, cores would be needed to determine which cutoff method gives optimum results for secondary porosity computation in the Asmari formation. The secondary porosity outputs by WN and TSR methods are displayed in the composite plot to represent possible mini-

mum and maximum limits of secondary porosity, respectively.

The secondary porosity (possibly due to dissolution) varies from 0 to 10% with some intervals showing higher secondary porosity than 10%. Such zones are not possibly showing realistic secondary porosity because it is affected by the input log porosity, which is raw cross-plot density-neutron porosity. The zones with broader porosity distribution are the one that computed higher secondary porosity. Such zones include: 1867-1874m, 1943-1947m, 1951-1953m, 1962-1965m, 1970.5-1973.5m, 1986.5-1988m, 1998-2001m, 2008-2022, 2038-2040m, 2043-2061m, 2067-2071m, 2075-2079m, 2090-2095m, 2116-2121m, 2137-2143m, 2150-2152m, 2162-2164m, 2170-2173m, 2214-2218m, 2255-2256.5m, 2303-2306m, 2313-2316m, 2326-2329m, 2424-2435m and 2437-2443m (Figures 9 & 10).

### (c) High-resolution porosity array & porosity VDL

It is obtained from the average of the porosity map

## Current Research Paper

/ histograms constructed from 192 porosity channels around the well bore. For the current well, it was output at 0.1 inch depth sampling. Based on their comparison with the effective log porosity and core porosity, following observations have been made:

High and low porosity layers / streaks of smaller thickness, not resolved by the conventional porosity logs, get highlighted on the high-resolution porosity. The high resolution FMI porosity tends to match with the cross-plot density-neutron porosity over the homogenous zones while it reads less than the log porosity over the heterogeneous intervals having broader porosity distribution.

Porosity histograms and VDL display indicates that more than half interval of Asmari formation is heterogeneous in terms of porosity distribution as indicated by wide porosity distribution. However, there are some zones which have narrow and dominantly unimodal distribution of porosity. Such zones include 1847-1867m, 1890-1941m, 2022-2037m, 2129-2136m, 2147-2162m, 2203-2209m, 2222-2226m, 2232-2236m, 2242-2259m, and 2316-2390m.

The importance to know the occurrence of high porosity streaks (which may also have high permeability) increases more when the field enters injection phase because such layers / streaks may cause

early break-through of injected water / gas from the injectors. Similarly the thin dense streaks / layers, which may go undetected with the conventional logging techniques, may act as barriers or baffles for the vertical flow of the reservoir fluids.

### Porosity analysis for the well number GS-B:

#### (a) Porosity system

The accuracy of porosity analysis from the image logs is largely dependent on the selection of right values for the parameters used in the analysis. Therefore some priori knowledge about the type and size of secondary pores is required for the rocks to be evaluated with the imaging tools. Since no core data was available for that purpose in the study well, therefore analysis was carried out in such a way that whole range of macro-secondary pores could be addressed. The porosity analysis was carried out to provide macro-secondary porosity (vugs / moulds) and high-resolution porosity for Asmari and Pabdeh formations. The porosity results (secondary porosity and high resolution porosity) are output at 0.1 inch and 1.5 inch. While the porosity histogram / VDL display is output at 1.5 inch. All porosity results (secondary porosity, porosity minimum and maximum limits, and high resolution porosity) from the study well are dis-

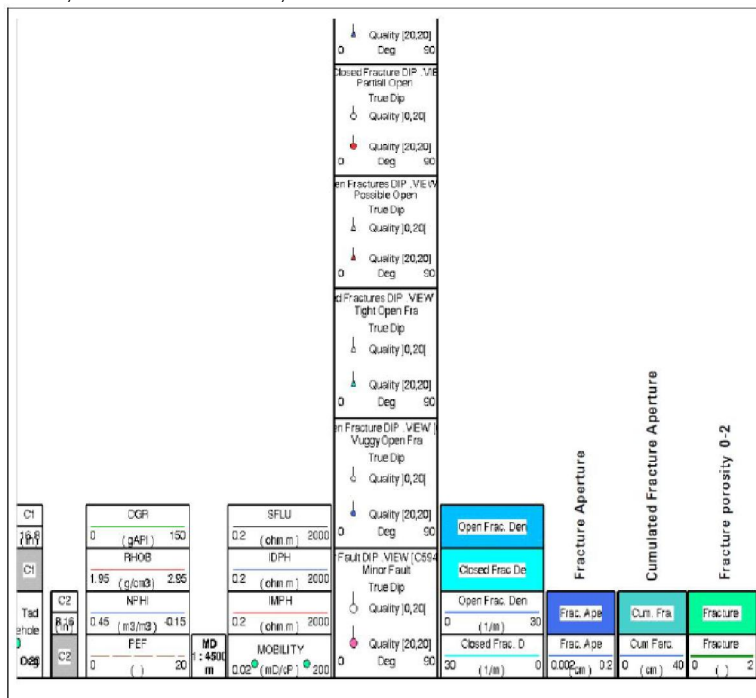


Figure 11 : Header for the summary plot of Figure 12

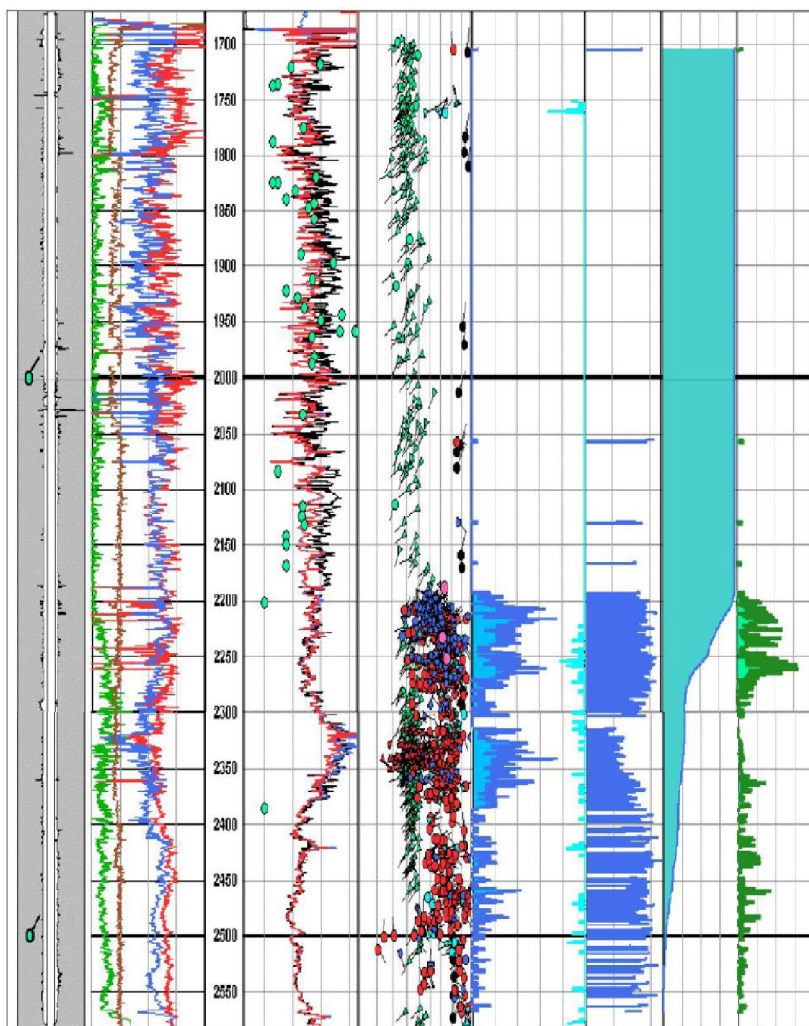


Figure 12 : Summary log of resistivity, density, porosity, dips, fractures density and apertures in Asmari, Pabdeh and Gurpi formations

TABLE 1 : Porosity distribution

Porosity Distribution		Secondary Porosity Intervals			Figures
Broad	Narrow	Porosity Range 2 – 5 %	Porosity Range 5 – 8 %	Porosity Range 8 % - Above	
1714-1732	1736-1820	1740-1820	1718-1725	1747-1749	Enclosure-1
1732-1736	1874-1886	1965-1960	1732-1738	1813-1815	
1820-1834	1928-1936	1996-2044	1820-1854	1819-1821	
1836-1874		2052-2082	2045-2053	1895-1903	
1886-1928		2154-2164	2080-215-	1927-1930	
1936-1964		2190-2198	2174-2182	1955-1960	
1986-1994		2220-2240	2198-2115	2186-2199	
2044-2052		2256-2348	2348-2363	2211-2213	
2084-2186		2380-2570			

played at 1.5 inch in the (Figures 11 & 12). The results of porosity analysis are discussed in the following.

(b) Vuggy / mouldic porosity

The secondary porosity (possibly due to dissolu-

## Current Research Paper

tion) varies from 1 to 20% with some intervals showing higher secondary porosity than 20%. The secondary porosity in the study well is largely affected by the image quality; hence cannot be used as such for quantitative purposes. The image quality is affected mainly by the badhole in some places, by the change of oil-base mud to oil-water emulsions, and by the presence of shale / clays particularly in Pabdeh and Gurpi. So the secondary porosity in this case can be used only in qualitative sense for comparing one zone with the other.

The intervals with broader porosity distribution are the heterogeneous ones and they computed higher secondary porosity. Intervals having various range of secondary porosity are given in the following table to highlight the zones of higher possible productivity associated with higher amount of secondary / dissolution pores (TABLE 1).

### (c) High-resolution porosity array & porosity VDL

It is obtained from the average of the porosity map / histograms constructed from 192 porosity channels around the well bore. For the current well, it was out-

put at 0.1 inch depth sampling. Based on their comparison with the effective log porosity and core porosity, following observations have been made (Figures 13 & 14):

High and low porosity layers / streaks of smaller thickness, not resolved by the conventional porosity logs, get highlighted on the high-resolution porosity. The high resolution FMI porosity tends to match with the cross-plot density-neutron porosity over the homogeneous zones while it reads less than the log porosity over the heterogeneous intervals having broader porosity distribution.

Porosity histograms and VDL display indicates that more than half interval of Asmari formation is heterogeneous in terms of porosity distribution as indicated by wide porosity distribution. However, there are some zones, which have narrow, and dominantly unimodal distribution of porosity. Such zones include: 1706-1818m, 1924-1932m, 1961-1986m, 1994-2035m, 2052-2084m, and 2186-2240m. The VDL image shows, Pabdeh and Gurpi Formations are homogeneous in terms of porosity distribution.

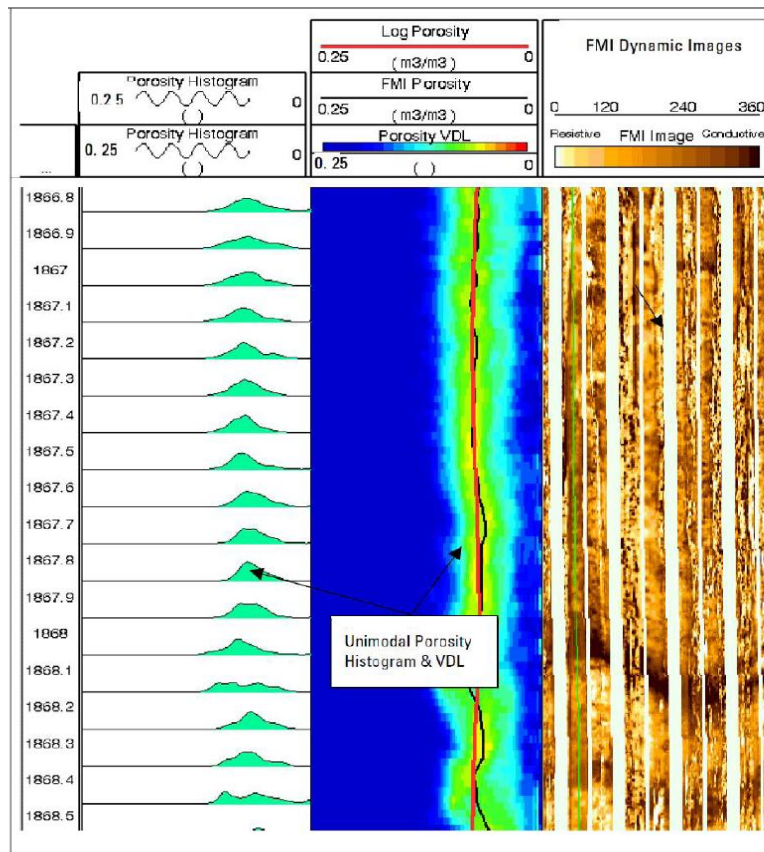


Figure 13 : Narrow range of porosity shown by porosity-VDL (variable-density-log) and porosity-histograms in a section of Asmari indicates its homogeneous nature

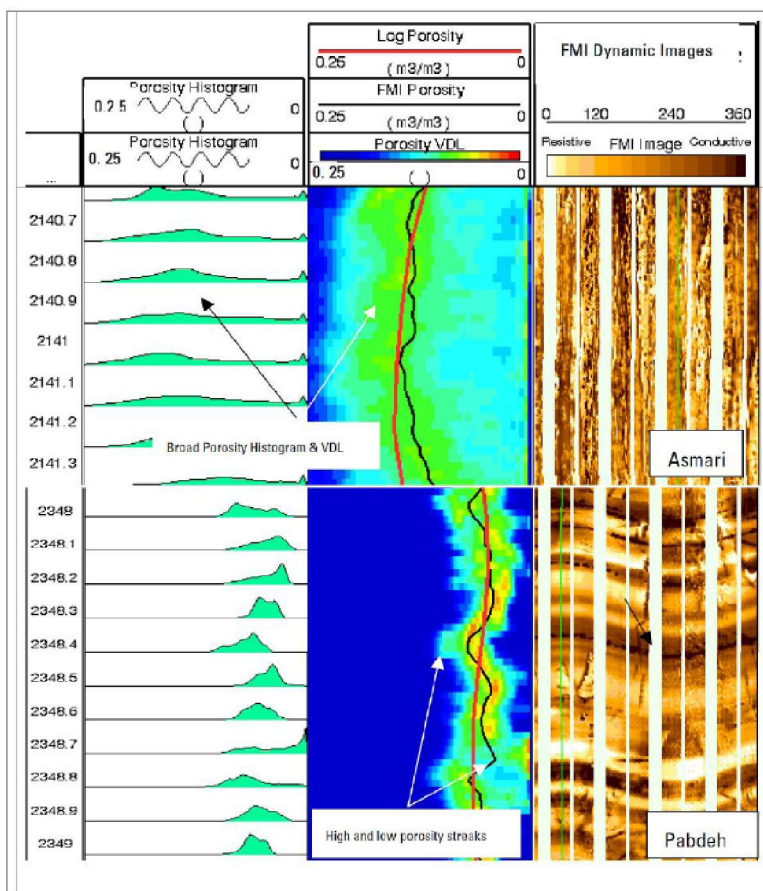


Figure 14 : Porosity VDL (variable-density-log) and histogram display over sections of Asmari and Pabdeh formations. The section from Asmari formation is showing broad distribution, which is a result of bad quality image affected by bad borehole conditions. High and low porosity streaks are indicated by porosity VDL and average porosity curve (black)

## CONCLUSION

This work shows how image log technology can be used to do the porosity analysis in oil and gas reservoirs. It is an example of porosity analysis that we did in Gachsaran field, located in South of Iran. In this paper, we describe the method in which we can find out detailed information about the porosity system in oil and gas reservoirs.

## REFERENCES

- [1] F.Khoshbakht, H.Memarian, M.Mohammadnia; Comparison of Asmari, Pabdeh and Gurpi formation's fractures, derived from image log, *J.Petrol.Sci.Eng.*, doi: 10.1016/j.petrol.2009.02.011, **67(1-2)**, 65-74 (2009).
- [2] Z.Movahed, R.Junin, Z.Safarkhanlou, M.Akbar;

- Formation evaluation in Dezful embayment of Iran using oil-based-mud imaging techniques, *J.Petrol.Sci.Eng.*, doi: 10.1016/j.petrol.2014.05.019i, **121**, 23-37 (2014).
- [3] Z.Movahed; Enhanced Reservoir Description in Carbonate and Clastic Reservoirs, Paper presented at the SPE Asia Pacific oil & Gas Conference and Exhibition, Jakarta, Indonesia, 30 October-1 November. <http://www.tmt-upn.blogspot.com/2007/10/spe-asia-pacific-oil-gas-conference.html> (2007).
- [4] F.Khoshbakht, M.Azizzadeh, H.Memarian, G.H.Nourozi, S.A.Moallemi; Comparison of electrical image log with core in a fractured carbonate reservoir, *J.Petrol.Sci.Eng.*, doi: 10.1016/j.petrol.2012.03.007, **86-87**, 289-296 (2012).